Inorg. Chem. **1987**, *26*, 944–948

Contribution from the Department of Chemistry and Molecular Structure Center,
Indiana University, Bloomington, Indiana 47405

A Binuclear Vanadium(III) Complex Containing the Linear $[VOV]^{4+}$ Unit: Preparation, Structure, and Properties of $[V_2O(SCH_2CH_2NMe_2)_4]$

Joanna K. Money, Kirsten Folting, John C. Huffman, and George Christou*

Received October 2, 1986

The synthesis, structure, and properties of $V_2O(Me_2\text{-aet})_4$ (Me_2-aet is 2-(dimethylamino)ethanethiolate) are reported. The synthesis and properties of corresponding $V_2O(\text{aet})_4$ (aet is 2-aminoethanethiolate) are also described. $V_2O(Me_2\text{-aet})_4\cdot$toluene$\cdot$THF crystallizes in triclinic space group $P\bar{1}$ with the following unit cell dimensions (at ~−154 °C): $a = 12.156$ (4), $b = 14.379$ (4), $c = 11.521$ (3) Å; $\alpha = 113.57$ (1), $\beta = 104.70$ (2), $\gamma = 66.07$ (1)°; $Z = 2$. The molecule possesses an essentially linear V–O–V bridging unit (177.84 (25)°). Each V is in approximate trigonal-bipyramidal coordination geometry with the bridging O and two thiolate S atoms occupying equatorial positions and two N atoms in the axial positions. The N–V–N axes at the two ends of the molecule are staggered (torsional angles 89.26–90.57°) to yield a molecule with idealized S_4 symmetry. The electronic makeup of the dimer has been probed by a Fenske–Hall molecular orbital calculation and compared to that of the corresponding hypothetical complex with equatorial rather than axial N atoms. The axial situation is shown to be favored because it optimizes V–N σ and V–S π overlaps. Electrochemical and UV/vis data are also described. The conversion of $VO(\text{aet})_2$ to $V_2O(\text{aet})_4$ has been accomplished by using sodium acenaphthylenide and aetH·HCl, the latter to function as a proton source. This result suggests that VO^{2+} impurities of crude oils may initially be converted to $[V\text{–}O\text{–}V]^{4+}$ or non-oxo-containing species under the reducing conditions employed in crude oil hydrodesulfurization.

Introduction

The chemistry of vanadium with oxygen exists predominantly for the higher oxidation states of the metal. There are many examples known of complexes containing the vanadyl $(V{=}O)^{2+}$ unit in its characteristic square-pyramidal or distorted-octahedral geometry.[1-9] Dinuclear and polynuclear oxygen-bridged compounds are seen in the oxides[10,11] and also the vanadates in aqueous solution.[12,13] There are also a few examples of these types of compounds in nonaqueous media.[7,13,14] For V(III), the presence of a V(III)–O–V(III) unit is rare. It is known to exist fleetingly in aqueous perchlorate solutions,[15] and $[H_2O(CH_3COO)V\text{–}O\text{–}V(CH_3COO)_2]^+$ has been observed at low pH in acetate media.[16] To date, the only structurally characterized example is $[(THF)_3Cl_2VOVCl_2(THF)_3]$, an isolable intermediate formed during the reduction of VCl_3 by triethylaluminum in tetrahydrofuran (THF).[17]

There are no characterized examples of $[V\text{–}O\text{–}V]^{4+}$ linkages with sulfur and/or nitrogen ligands. Compounds of this type can be considered as viable models of intermediates in the formation of V_xS_y polymers during the hydrodesulfurization (HDS) of crude oils. The heavier crudes, which are now more commonly being processed, contain large amounts of vanadium, primarily as VO^{2+} species. These VO^{2+} species exist in either a porphyrin or non-porphyrin environment.[18] EPR studies indicate that the first coordination sphere of the non-porphyrin species consists of a mixture of N, S, and/or O ligation.[19] These compounds react with H_2/H_2S during the HDS process to form vanadium(III) sulfide polymers, which poison the Co–Mo catalyst.[20,21] It is possible that one of the initial steps in the formation of these polymers is the reduction of the metal center and formation of higher nuclearity species.

One objective of our research has been the preparation and characterization of soluble models of these intermediate species with the metal being in a whole or partial sulfur environment. There is only one other characterized example of a V(III) complex with thiolate ligation, namely $[V_2(\text{edt})_4]^{2-}$ (edt is ethane-1,2-dithiolate), a dimer with four bridging S atoms where each V possesses one terminal dithiolate and shares two bridging dithiolates with the other vanadium.[22] As part of our continuing investigation of this chemistry, we have examined the effect of varying the ligand type. We have chosen for study the N,S-ligand 2-aminoethanethiolate, where one $-S^-$ of the edt group has been substituted by an $-NR_2$ moiety (R = H, Me). We herein report the results of this investigation, the synthesis and characterization of a rare example of a compound containing a linear $[VOV]^{4+}$ bridging unit.

Experimental Section

All manipulations were performed by using standard inert-atmosphere techniques and a dinitrogen atmosphere. Solvents were purified by distillation from CaH_2 (MeCN) or Na/benzophenone (THF, toluene, Et_2O, hexanes); other solvents were dried over molecular sieves. All solvents were thoroughly degassed before use. 2-Aminoethanethiol (aetH) and 2-(dimethylamino)ethanethiol (Me_2-aetH) were purchased as the hydrochloride salts and recrystallized from $EtOH/Et_2O$ before use. VCl_3 was used as received.

$V_2O(\text{aet})_4\cdot 2DMF$ (1). A solution of Na(aet) was prepared by dissolving sodium metal (1.38 g, 60 mmol) in MeOH (25 mL) and adding aetH·HCl (3.41 g, 30 mmol). The solvent was removed in vacuo and MeCN (100 mL) added to the white solid. Solid VCl_3 (1.57 g, 10 mmol) was added to the white slurry and the mixture stirred. The reactants dissolved to give a brown solution that soon began to deposit a brown

---

(1) Selbin, J. *Chem. Rev.* **1965**, *65*, 153; *Coord. Chem. Rev.* **1966**, *1*, 293.
(2) Bruins, D.; Weaver, D. L. *Inorg. Chem.* **1970**, *9*, 130.
(3) Henrick, K.; Raston, C. L.; White, A. H. *J. Chem. Soc., Dalton Trans.* **1976**, 26.
(4) Tapscott, R. E.; Belford, R. L.; Paul, I. C. *Inorg. Chem.* **1968**, *7*, 356.
(5) Money, J. K.; Huffman, J. C.; Christou, G. *Inorg. Chem.* **1985**, *24*, 3297.
(6) Form, G. E.; Raper, E. S.; Oughtred, R. E.; Shearer, H. M. M. *J. Chem. Soc., Chem. Commun.* **1972**, 945.
(7) Cotton, F. A.; Lewis, G. E.; Mott, G. N. *Inorg. Chem.* **1982**, *21*, 3127 and 3316.
(8) Weighardt, K.; Bossek, U.; Volckmar, K.; Swiridoff, W.; Weiss, J. *Inorg. Chem.* **1984**, *23*, 1987.
(9) Densar, A.; Bukovec, P. *J. Fluorine Chem.* **1984**, *24*, 369.
(10) Selbin, J.; Holmes, L. H. *J. Inorg. Nucl. Chem.* **1962**, *24*, 1111.
(11) Evans, H. T.; Swallow, A. G.; Barne, W. H. *J. Am. Chem. Soc.* **1975**, *86*, 4209.
(12) Nawmann, A. W.; Hallada, G. J. *Inorg. Chem.* **1964**, *3*, 70.
(13) Halko, D. J.; Swinehart, J. H. *J. Inorg. Nucl. Chem.* **1979**, *41*, 1589.
(14) Murmann, R. K. *Inorg. Chim. Acta* **1977**, *25*, L43.
(15) Newton, T. W.; Baker, F. B. *Inorg. Chem.* **1964**, *3*, 569.
(16) Gandeboeuf, J.; Souchag, P. *J. Chim. Phys. Phys.-Chim. Biol.* **1959**, *56*, 358.
(17) Chandrasekhar, P.; Bird, P. H. *Inorg. Chem.* **1984**, *23*, 3677.
(18) Biggs, W. R.; Fetzer, J. C.; Brown, R. J.; Reynolds, J. G. *Liq. Fuels Technol.* **1985**, *3*, 397.
(19) Reynolds, J. G., personal communication. Reynolds, J. G.; Gallegos, E. J.; Fish, R. H.; Komlenic, J. J. *Liq. Fuels Technol.*, in press.
(20) Silbernagel, B. G. *J. Catal.* **1979**, *56*, 315.
(21) Tamm, P. W.; Harnsberger, H. F.; Bridge, A. G. *Ind. Eng. Chem. Process Des. Dev.* **1981**, *20*, 262.
(22) Wiggins, R. W.; Huffman, J. C.; Christou, G. *J. Chem. Soc., Chem. Commun.* **1983**, 1313. Dorfman, J. R.; Holm, R. H. *Inorg. Chem.* **1983**, *22*, 3179. Szeymies, D.; Krebs, B.; Henkel, G. *Angew. Chem. Suppl.* **1983**, 1176.

0020-1669/87/1326-0944$01.50/0

Table I. Crystallographic Data for **2**·$PhCH_3$·THF

formula	$C_{27}H_{56}N_4O_2S_4V_2$
mol mass, g·mol^{-1}	698.89
crystal system	triclinic
space group	$P\bar{1}$
temp, °C	−154
a, Å	12.156 (4)[a]
b, Å	14.379 (4)
c, Å	11.521 (3)
α, deg	113.57 (1)
β, deg	104.70 (2)
γ, deg	66.07 (1)
Z	2
vol, Å^3	1676.94
radiation	Mo Kα (0.71069 Å)[b]
abs coeff, cm^{-1}	8.083
crystal size, mm	0.40 × 0.36 × 0.36
scan speed, deg min^{-1}	4.0
scan width, deg	1.8 + dispersion
scan range, deg	$6 \le 2\theta \le 45$
no. of total data	4513
no. of unique data	4403
averaging R[c]	0.021
no. of obsd data	3691, $F > 3\sigma(F)$
R, %	5.87[d]
R_w, %	6.28[e]
goodness of fit	1.473[f]

[a] 32 reflections at −154 °C. [b] Graphite monochromator. [c] 42 reflections measured more than once. [d] $R = \sum||F_o| - |F_c||/\sum|F_o|$. [e] $R_w = [\sum w(|F_o| - |F_c|)^2/\sum w|F_o|^2]^{1/2}$ where $w = 1/\sigma^2(|F_o|)$. [f] Goodness of fit $= [\sum w(|F_o| - |F_c|)^2/(N_{obsns} - N_{params})]^{1/2}$.

solid. Precipitation was complete after about 30 min. The solid was collected by filtration, washed with MeCN and Et_2O, and dried in vacuo. Recrystallization from warm DMF yielded long, thin fiberlike crystals in ~35% yield. Anal. Calcd for $C_{14}H_{38}N_6O_3S_4V_2$: C, 29.57; H, 6.74; N, 14.78. Found: C, 28.84; H, 7.17; N, 14.57.

$V_2O(Me_2$-aet$)_4$ (2). A slurry of Na(Me_2-aet) in MeCN (100 mL) was prepared as described above for Na(aet). Solid VCl_3 (1.57 g, 10 mmol) was added, and on stirring, a dark brown solution was obtained. A white solid (NaCl) was removed by filtration and the volume of the filtrate reduced by half. Overnight storage of this solution at −20 °C yielded dark brown crystals, which were collected by filtration and dried in vacuo. Recrystallization can be effected from warm toluene or THF/hexanes to yield well-formed prisms that convert to a powder on drying in vacuo. Analysis of the powder indicates the nonsolvated form. Anal. Calcd for $C_{16}H_{40}N_4OS_4V_2$: C, 35.94; H, 7.54; N, 10.48; S, 23.99. Found: C, 35.56; H, 7.47; N, 10.40; S, 23.90. The crystallographic sample was recrystallized twice, first from THF/hexanes and then from warm toluene. The brown prisms were kept in contact with the mother liquor until a suitable crystal was chosen and transferred to the goniostat. Electronic spectrum in MeCN [λ_{max}, nm (ϵ_M, L·mol^{-1}·cm^{-1})]: 807 (850), 463 (12750), 324 (9500), 240 (23840).

VO(aet)$_2$ (3). This known compound was prepared by a procedure modified from that reported previously.[23] Sodium metal (0.92 g, 40 mmol) was dissolved in EtOH (80 mL) and aetH·HCl (2.27 g, 20 mmol) added to give a white slurry. On addition of VO(acac)$_2$ (2.65 g, 10 mmol), the white solid began to dissolve and was replaced by a fine purple precipitate. After the reaction mixture was stirred for 30 min, the product was collected by filtration, washed with EtOH, and dried in vacuo. Recrystallization from warm DMF/Me_2SO/EtOH gave deep purple prisms in ~40% overall yield; ν(V=O) 967 cm^{-1}.

Conversion of VO(aet)$_2$ to V_2O(aet)$_4$. A solution of compound **3** (0.31 g, 1.40 mmol) and aetH·HCl (0.185 g, 1.63 mmol) in DMF (10 mL) was treated with a 0.1 M solution of sodium acenaphthylenide (18 mL, 1.80 mmol) in THF. The solution color rapidly changed from purple to brown. Some molecular sieves were added to the solution and the flask then stored overnight at −20 °C. The resulting brown solid was collected by filtration and recrystallized from warm DMF to give thin brown crystals in ~40% yield. The IR spectrum of this solid was identical with that of an authentic sample of **1**.

X-ray Crystallography and Structure Solution. Data were collected at approximately −154 °C on a Picker four-circle diffractometer; full details of the diffractometry, low-temperature facilities, and computational procedures employed by the Molecular Structure Center are available elsewhere.[24] Data collection parameters are summarized in Table I.

A systematic search of a limited hemisphere of reciprocal space yielded a set of reflections that exhibited no symmetry or extinctions. The choice of the centrosymmetric space group $P\bar{1}$ was confirmed by the successful solution and refinement of the structure.

The structure was solved by a combination of direct-methods (MULTAN) and Fourier techniques. After location of the vanadium dimer and toluene solvate, a seriously disordered THF molecule was found lying on a center of symmetry. Only the carbon atoms of the latter molecule were clearly observable, and these were included in the refinement cycles with isotropic thermal parameters, all other non-hydrogen atoms being refined with anisotropic thermal parameters. In the latter stages, all hydrogen atoms, except those of the THF molecule, were located and included in refinement cycles with isotropic thermal parameters. In the final refinement cycle, a peak close to the THF carbon atoms was located, situated near the center of symmetry; this was assigned as the THF oxygen atom completing the five-membered ring but was not included in the refinement due to its poor behavior. Final values of discrepancy indices R and R_w were quite satisfactory and are included in Table I.

Molecular Orbital Calculations. Calculations were performed by the Fenske–Hall method (program Medieval)[25] at the Indiana University Computational Chemistry Center, using a VAX 11/780 computer system.

All atomic wave functions were generated by a best fit to Hermann–Skillman atomic calculations using the method of Bursten, Jensen, and Fenske.[26] Contracted double-ζ representations were used for V 3d as well as N and O 2p AO's and S 3p AO's. Basic functions for the metal atoms were derived for a +1 oxidation state with the valence s and p exponents fixed at 1.95 for V 4s and 4p orbitals.[27] An exponent of 1.16 was used for the H 1s atomic orbital.[28]

Averaged bond lengths were obtained from the X-ray structure determination of $V_2O(Me_2$-aet$)_4$. To simplify the calculations, the CH_2 groups on N and S and CH_3 groups on the N were replaced with hydrogen atoms. An S–H bond length of 1.34 Å, an N–H bond length of 1.00 Å, a V–S–H angle of 120°, and a V–N–H angle of 109.5° were used. The geometry around each metal atom was idealized to trigonal bipyramidal, and the ligands on one V were staggered with respect to the other V. The geometry at N was tetrahedral. The coordinate system oriented the z axis along the V–O–V vector and put the axial ligands along the x and y axes. Calculations were carried out on conformers A and B; in A the nitrogen atoms were in the axial positions, and in B the sulfurs were axial.

Other Measurements. Infrared spectra were recorded as Nujol mulls on a Perkin-Elmer Model 283 spectrophotometer. Electronic spectra were obtained in DMF and MeCN solutions for **1** and **2**, respectively, on a Perkin-Elmer Model 330 spectrophotometer. Electrochemical measurements were performed in the cyclic voltammetry (CV) mode with an IBM Model EC 225 voltammetric analyzer using a glassy-carbon working electrode, a Pt-wire auxiliary electrode, and an SCE reference electrode. The supporting electrolyte was 0.1 M N(n-Bu)$_4$ClO$_4$ (TBAP), and concentrations of electroactive species were ca. 4 mM. Measurements were performed in MeCN, CH_2Cl_2, and THF for **2** and DMF for **1**, and potentials are quoted vs. the normal hydrogen electrode (NHE) using ferrocene as an external standard ($E_{1/2}$ = +0.400 V vs. NHE).[29] No iR compensation was employed.[29] Magnetic moments were determined on powdered samples by using a Johnson Matthey magnetic susceptibility balance and on C_6D_6 solutions by using the Evans NMR method with hexamethyldisiloxane as the reference peak. Diamagnetic corrections using Pascal's constants were employed.

Results and Discussion

Synthesis and Crystal Structure. Our work with the aet$^-$ ligand was an extension to earlier studies[22] employing edt^{2-}. The latter ligand had been shown to react with VCl_3 in alcohol to yield intensely colored solutions containing the $[V_2(edt)_4]^{2-}$ anion, whose structure consists of an unusual quadruply bridged $[V_2(edt)_2]^{2+}$

---

(23) Hodge, A.; Nordquest, K.; Blinn, E. L. *Inorg. Chim. Acta* **1972**, *6*, 491.

(24) Chisholm, M. H.; Folting, K.; Huffman, J. C.; Kirkpatrick, C. C. *Inorg. Chem.* **1984**, *23*, 1021.

(25) Hall, M. B.; Fenske, R. F. *Inorg. Chem.* **1972**, *11*, 768.

(26) Bursten, B. E.; Jensen, J. R.; Fenske, R. F. *J. Chem. Phys.* **1978**, *68*, 3320.

(27) Valence s and p orbital exponents of 1.95 kept the populations of V 4s orbitals less than 0.25 and 4p orbitals less than 0.1.

(28) Hehre, W. J.; Steward, R. F.; Pople, J. A. *J. Chem. Phys.* **1969**, *51*, 2657.

(29) Gagne, R. G.; Koval, C. A.; Lisensky, G. C. *Inorg. Chem.* **1980**, *19*, 2855.

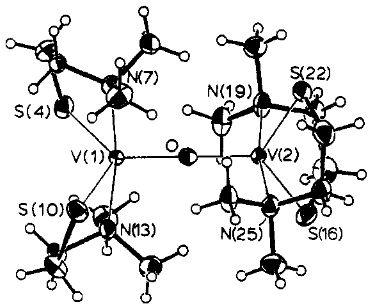

Figure 1. ORTEP projection and labeling scheme for **2**. Non-hydrogen atoms are depicted as 50% probability ellipsoids; hydrogen atoms are depicted as spheres of arbitrary size.

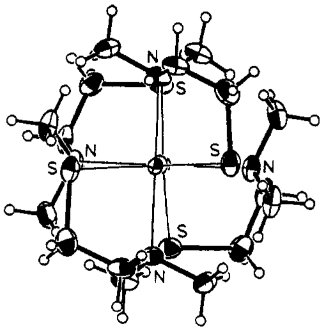

Figure 2. ORTEP projection of **2** viewed down the V–O–V axis. For clarity, only S and N atoms are labeled.

core with four μ-sulfur atoms. In addition, the V···V separation (2.600 (2) Å) was indicative of direct metal–metal bonding. Wondering to what extent this unusual arrangement was dependent on the edt^{2-} ligand, we decided to investigate similar reactions with aet$^-$, which possesses the same chain length as edt^{2-}. Initial reactions were in EtOH and, subsequently, in MeCN; in both cases, addition of VCl_3 to 3 equiv of Na(aet) resulted in the rapid precipitation of **1** as a brown powder soluble only in warm DMF. Recrystallization from DMF or DMF/Et_2O yielded fibrous crystals unsuitable for structural studies. To increase product solubility and, hopefully, improve the crystal form, the ligand Me_2-aet$^-$ was employed. The resulting reaction yielded **2**, but now the product was much more soluble (DMF, MeCN, Me_2CO, CH_2Cl_2, THF, Et_2O, toluene) and gave well-formed prisms on recrystallization suitable for crystallography. The structural studies (vide infra) identified **2** as $V_2O(Me_2\text{-aet})_4$; spectroscopic comparisons and elemental analysis identified **1** as $V_2O(aet)_4$. The crystallographic sample was recrystallized twice (see Experimental Section) and was found to also contain a toluene and, surprisingly, a THF molecule, the latter being obviously carried over from the first recrystallization.

With the identity of **2** established, the question arose as to the origin of the bridging oxygen atom. Adventitious water, O_2, or even alcohol molecules were considered likely candidates; note that reactions in MeCN used ligands that had been deprotonated in MeOH so that traces of the latter may have still been present. We thus prepared solid, dry Na(aet) by reaction of aetH·HCl with 1 equiv of Na metal in THF; precipitated NaCl was removed by filtration and then a second equivalent of Na metal added to yield a precipitate of Na(aet). When this dried material was reacted with VCl_3 in a glovebox in freshly distilled, degassed MeCN, a much slower reaction occurred, but this again led to precipitation of **1**. No sign of any intermediate $[V_x(aet)_y]^z$ species likely to correspond to $[V_2(edt)_4]^{2-}$ was observed. We conclude that **1** is the only detectable product and that this is formed from adventitious O-containing impurities in the solvent, reagents, or N_2 atmosphere.

Table II. Fractional Coordinates and Isotropic Thermal Parameters for **2**[a]

atom	x	y	z	B_{iso}, Å^2
V(1)	2631 (1)	1309 (1)	3212 (1)	13
V(2)	1320 (1)	2785 (1)	988 (1)	13
O(3)	1953 (3)	2038 (3)	2102 (3)	22
S(4)	4509 (1)	−45 (1)	2872 (2)	24
C(5)	5507 (6)	657 (6)	4059 (7)	29
C(6)	4796 (6)	1660 (5)	5042 (6)	27
N(7)	3733 (4)	2342 (4)	4450 (4)	21
C(8)	3084 (6)	3278 (5)	5511 (7)	30
C(9)	4098 (6)	2770 (5)	3715 (6)	25
S(10)	1658 (1)	1662 (1)	4932 (1)	26
C(11)	1130 (6)	497 (6)	4328 (7)	32
C(12)	1701 (6)	−348 (5)	3168 (6)	26
N(13)	1667 (4)	126 (4)	2216 (5)	22
C(14)	2243 (6)	−771 (5)	1108 (6)	27
C(15)	393 (6)	671 (6)	1793 (6)	26
S(16)	80 (1)	2223 (1)	−858 (1)	23
C(17)	1143 (6)	1607 (5)	−2057 (6)	27
C(18)	2268 (6)	1916 (5)	−1541 (6)	23
N(19)	2780 (4)	1781 (4)	−284 (5)	20
C(20)	3879 (6)	2107 (6)	166 (7)	31
C(21)	3179 (6)	622 (5)	−424 (6)	30
S(22)	1735 (1)	4348 (1)	1448 (2)	25
C(23)	301 (7)	5391 (5)	2014 (7)	31
C(24)	−684 (6)	4919 (5)	1674 (6)	27
N(25)	−289 (4)	3935 (4)	2031 (5)	22
C(26)	−1332 (6)	3547 (6)	1675 (7)	31
C(27)	43 (6)	4190 (6)	3404 (6)	32
C(28)′	7415 (6)	2114 (6)	3400 (7)	33
C(29)′	6751 (7)	2342 (7)	2326 (8)	41
C(30)′	6037 (8)	3391 (7)	2387 (8)	43
C(31)′	6040 (8)	4202 (7)	3567 (10)	47
C(32)′	6706 (6)	3976 (6)	4626 (8)	34
C(33)′	7416 (7)	2929 (6)	4567 (8)	39
C(34)′	8132 (8)	2674 (8)	5711 (9)	53
C(35)″	5779 (9)	5423 (9)	257 (10)	60 (2)
C(36)″	3954 (11)	6314 (10)	1526 (12)	79 (3)
C(37)″	5222 (14)	6295 (12)	1198 (15)	113 (4)
C(38)″	5851 (15)	4607 (15)	−605 (17)	117 (4)

[a] Coordinates are ×10^4. B_{iso} values are ×10. Primed and double-primed atoms refer to toluene and THF solvate molecules, respectively.

Table III. Selected Bond Lengths (Å) and Angles (deg)

a. Bonds			
V(1)–S(4)	2.3219 (20)	V(2)–S(16)	2.3318 (19)
V(1)–S(10)	2.3411 (19)	V(2)–S(22)	2.3286 (20)
V(1)–O(3)	1.803 (4)	V(2)–O(3)	1.822 (4)
V(1)–N(7)	2.233 (5)	V(2)–N(19)	2.222 (5)
V(1)–N(3)	2.226 (5)	V(2)–N(25)	2.232 (5)
b. Angles			
S(4)–V(1)–S(10)	119.83 (7)	S(16)–V(2)–S(22)	119.65 (7)
S(4)–V(1)–O(3)	118.11 (14)	S(16)–V(2)–O(3)	121.33 (14)
S(4)–V(1)–N(7)	83.64 (14)	S(16)–V(2)–N(19)	83.29 (14)
S(4)–V(1)–N(13)	91.96 (14)	S(16)–V(2)–N(25)	91.28 (14)
S(10)–V(1)–O(3)	122.05 (14)	S(22)–V(2)–O(3)	119.01 (14)
S(10)–V(1)–N(7)	91.66 (14)	S(22)–V(2)–N(19)	92.51 (14)
S(10)–V(1)–N(13)	82.85 (14)	S(22)–V(2)–N(25)	83.37 (14)
O(3)–V(1)–N(7)	95.75 (18)	O(3)–V(2)–N(19)	95.23 (18)
O(3)–V(1)–N(13)	94.12 (18)	O(3)–V(2)–N(25)	94.26 (18)
N(7)–V(1)–N(13)	170.13 (18)	N(19)–V(2)–N(25)	170.49 (18)
V(1)–O(3)–V(2)	177.84 (25)		

Complex **2** crystallizes in triclinic space group $P\bar{1}$ and contains discrete $V_2O(Me_2\text{-aet})_4$ units. Fractional coordinates and bond distances and angles are listed in Tables II and III, respectively. ORTEP projections are shown in Figures 1 and 2. The toluene and disordered THF molecules are well separated from the metals and will not be further discussed. The dimer contains a V–O–V bridging unit that is essentially linear (177.84 (25)°). The metals are five-coordinate and possess slightly distorted trigonal-bipyramidal geometry; N atoms occupy the axial positions (N–V–N = 170.13, 170.49°), and the bridging O and two thiolate S atoms occupy the equatorial positions. Equatorial–equatorial and axial–equatorial angles are in the ranges 118.11–122.05° and 82.85–95.75°, respectively, close to ideal values of 120 and 90° for a trigonal bipyramid. The two ends of the molecule are almost perfectly staggered, presumably to minimize steric interactions between the Me groups, with N–V–V–N torsional angles in the narrow range 89.26–90.57°. This yields a molecule of S_4 symmetry as emphasized by the view down the V–O–V axis shown in Figure 2. The V–O bond lengths (1.803, 1.822 Å) are longer than the ~1.6-Å bond length found in the oxovanadium(IV) (VO^{2+}) multiply bonded unit[1,5] but shorter than the ~1.9–2.1 Å values characteristic of V–O single bonds at this oxidation level.[7,30,31] This is consistent with a V–O bond order greater than 1, a conclusion that is in accord with the linearity of the bridge, which is itself characteristic of V d_π–O p_π bonding. In $V_2OCl_4(THF)_6$[17] the linear V–O–V bridge has V–O bond lengths of 1.769 (5) Å. Many other complexes containing linear M–O–M bridges are known in transition-metal chemistry, and short M–O bond lengths compared to single-bond values have been considered evidence for multiple bonding.[32] It should be noted that the majority of these species contain octahedrally coordinated metal centers; complex **2** represents a rare example of a linear M–O–M bridge between two five-coordinate metal centers.

Molecular Orbital Calculations. We wished to attain two objectives from our molecular orbital calculations using the Fenske–Hall method: (i) to probe the electronic structure of complex **2** and (ii) to rationalize the observed location of N atoms in axial rather than equatorial positions. Simple qualitative arguments for (ii) suggest that axial S atoms would be less preferred, as this leads to direct competition for available d_π metal orbitals for π-bonding interactions, a situation that would not occur with the purely σ-bonding N atoms. However, in equatorial positions, S atoms are in competition with the O atom for π-bonding. Thus, we felt that qualitative arguments alone could not provide a satisfactory rationalization of the observed ligand arrangement. Two calculations were, therefore, carried out: in conformer A, the observed ligand arrangement was used, i.e. with N atoms axial; in B, the S atoms were placed in axial positions.

In both conformers, the electronic structures of the bridging regions are essentially identical and will be described first. The V–O–V σ-framework consists of overlap primarily between the metal d_{z^2} and O p_z orbitals. The V–O–V π-bonding framework consists of overlap of metal d_{xz}, d_{yz}, and O p_y, p_z orbitals to yield two degenerate three-center bonding molecular orbitals. The HOMO is an essentially degenerate pair of orbitals consisting of symmetric and antisymmetric combinations of metal d_{xy} orbitals that possess δ symmetry with respect to the molecular z (V–O–V) axis. Both of these orbitals are filled, leading to a singlet ground-state situation. Their overlap populations are zero, and there is no contribution from O atomic orbitals. In addition, the d_{xy} orbitals make no significant contribution to other MO's. Such a situation is akin to two filled, localized d_{xy} orbitals of a valence-bond description. The LUMO is also a nonbonding interaction consisting of a degenerate pair of orbitals arising from combination of a d_{xz} orbital of one V and an orthogonal d_{yz} from the other.

The preference for conformer A over conformer B can be rationalized by consideration of V–N, S interactions. In both conformers A and B, S and N have σ-bonding overlaps with an orbital of primarily metal $d_{x^2-y^2}$ origin. In conformer A, the overlap of the N p_z orbital (ligand p_z orbitals are directed toward the metals) is approximately equal to that of the S p_z orbital. In conformer B, however, overlap of the N p_z orbital is significantly reduced and is now approximately half that of the S p_z orbital. Since NH_3 is a pure σ donor, the V–N bonds are, thus, stronger in conformer A. Similarly, in A the S p_x and p_y orbitals are able to form good π-bonding overlaps with the d_{z^2} and d_{yz} orbitals of one V and d_{z^2} and d_{xz} of the other. In B, however, overlap of these S orbitals with metal orbitals is greatly reduced, enhancing slightly the contribution of d_{z^2}, d_{xz}, and d_{yz} orbitals to the V–O–V bonding framework. Overall, it would seem that conformer A is preferred because it allows better V–N σ- and V–S π-bonding interactions even though it weakens slightly the V–O–V bonds relative to B. These π-bonding interactions between S and the metal d_{z^2} and $d_{xz,yz}$ orbitals in A are probably the cause of the observed lengthening of V–O distances in **2** (~1.81 Å) relative to those in $V_2OCl_4(THF)_6$ (~1.77 Å), for as we have described, these metal orbitals are intimately involved in V–O–V σ- and π-bonding interactions, respectively. Note that these bond length differences cannot be due simply to the differing metal coordination numbers, for such arguments would suggest that the bond lengths of **2** should be the shorter.

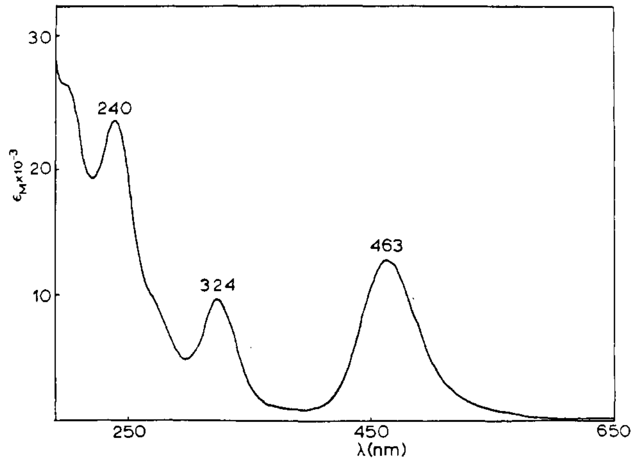

Figure 3. UV–visible absorption spectrum of **2** in MeCN solution.

Spectroscopic, Electrochemical, and Magnetic Studies. Newton and Baker first observed the $[V–O–V]^{4+}$ unit during a kinetic study of V(II) and V(IV) perchlorates in acidic media.[15] The $[V–O–V]^{4+}$ intermediate displayed an intense absorption at 425 nm. $[(H_2O)(CH_3COO)V–O–V(CH_3COO)_2]^+$ is also reported to display an identical absorption at 425 nm.[16] A similarly intense band is seen for $V_2OCl_4(THF)_6$ at 487 nm in THF and MeCN and at 482 nm in DMF.[17] The electronic spectrum of complex **2** in MeCN is shown in Figure 3 and displays a correspondingly intense band at 463 nm. The spectrum of **1** in DMF is very similar, with the band shifted slightly to 458 nm. This absorption is most likely due to a charge-transfer transition within the $[V–O–V]^{4+}$ unit.

Complex **2** exhibits an irreversible oxidation at –0.37 V vs. NHE in MeCN. No cathodic peak is seen in the cyclic voltammogram (CV) at 100 mV/s, a situation that persists in CH_2Cl_2 and THF, and at higher scan speeds. Complex **1**, however, shows a near-reversible oxidation ($i_a/i_c < 1$) at 100 mV/s ($E_{1/2} = -0.48$ V), which at 1 V/s approaches pseudoreversibility by electrochemical criteria ($i_a/i_c \approx 1$).

Complex **2** was found to be paramagnetic in solution, and an Evans NMR determination of its magnetic moment in C_6D_6 at ~23 °C yielded a value of 4.15 μ_B/V_2 (2.93 μ_B/V), consistent with expected values for a dinuclear species possessing four unpaired electrons (4.00 μ_B/V_2; 2.83 μ_B/V). Similar values were obtained in the solid state, precluding the possibility that in solution **2** yields two mononuclear vanadium(III) ($S = 1$) units. Since the MO calculation yields a singlet ground-state description, the paramagnetism is almost certainly due to thermal excitation of HOMO electrons into higher energy vacant orbitals. A better description of the magnetic properties of this system, however, must await a variable-temperature solid-state magnetic susceptibility study to very low temperatures.

Conversion of $VO(aet)_2$ (3) to $V_2O(aet)_4$ (1). As we noted in the Introduction, the oxovanadium(IV) impurities of crude oils are reduced and sulfided during HDS treatment to yield insoluble

---

(30) Cooper, S. R.; Koh, Y. B.; Raymond, K. N. *J. Am. Chem. Soc.* **1982**, *104*, 5092.

(31) Gambarotta, S.; Mazzanti, M.; Floriani, C.; Zehnder, M. *J. Chem. Soc., Chem. Commun.* **1984**, 1116.

(32) Broomhead, J. A.; Sterns, M.; Young, C. G. *Inorg. Chem.* **1984**, *23*, 729. Yevitz, M.; Stanko, J. A. *J. Am. Chem. Soc.* **1971**, *93*, 1512. DiVaira, M. D.; Mani, F. *Inorg. Chem.* **1984**, *23*, 409. Ziolo, R. F.; Stanford, R. H.; Rossman, G. R.; Gray, H. B. *J. Am. Chem. Soc.* **1974**, *96*, 7910. Schardt, B. C.; Hollander, F. J.; Hill, C. L. *J. Am. Chem. Soc.* **1982**, *104*, 3964. Vogt, L. H.; Zalkin, A.; Templeton, D. H. *Inorg. Chem.* **1967**, *6*, 1725. Yamada, S.; Katayama, C.; Tanaka, J.; Tanaka, M. *Inorg. Chem.* **1984**, *23*, 253. Herrmann, W. A. *Angew. Chem., Int. Ed. Engl.* **1986**, *25*, 56.

V(III) sulfide polymers, primarily V_2S_3. Elucidating possible intermediates represents one goal of our synthetic work. We can report that **3** can be cleanly converted to **1** in a controlled fashion under laboratory conditions, a result that suggests a similar reaction involving the conversion of VO^{2+} to $[V-O-V]^{4+}$ may be an initial step in the transformation of the crude oil impurities under the industrial conditions. Treatment of **3** with 1 equiv of sodium acenaphthylenide (NaACN) in the presence of aetH·HCl leads to a fairly rapid color change from purple to the brown that is characteristic of **1**. IR comparison of the isolated, recrystallized (DMF) solid with an authentic sample of **1** confirmed the identity of this product. The presumed stoichiometry of this conversion is indicated in eq 1. The simplified form of this equation is given

$$2VO(aet)_2 + 2aetH{\cdot}HCl + 2NaACN \rightarrow V_2O(aet)_4 + 2aetH + H_2O + 2ACN + 2NaCl \qquad (1)$$

in eq 2. In essence, reduction of **3** presumably yields $[VO(aet)_2]^-$,

$$2VO^{2+} + 2H^+ + 2e^- \rightarrow [V-O-V]^{4+} + H_2O \qquad (2)$$

which, in the presence of a proton source (aetH·HCl), dimerizes to **1** with elimination of H_2O. The $V{=}O^{2+}$ multiple bond would be expected to be seriously weakened and destabilized by lowering of the metal oxidation state.

If we entertain a little further the hypothesis that $[V-O-V]^{4+}$ species are formed from VO^{2+} in the industrial process, it is possible that reaction with H_2S will then yield $[V-S-V]^{4+}$ species followed by an increase in the S content with loss of peripheral ligation. We are currently investigating, therefore, whether $V_2O(aet)_4$ can be converted to $V_2S(aet)_4$.

Substitution of $(NMe_4)Na[VO(edt)_2]{\cdot}2EtOH$ and 2 $(Et_3NH)Cl$ for $VO(aet)_2$ and aetH·HCl in the reaction of eq 1 in MeCN leads to a brown crystalline product. The complex nature of this material has necessitated its elucidation by X-ray crystallography, which shows it to be the mixed-anion salt $(NMe_4)_6[VO(edt)_2]_2[V_2(edt)_4]{\cdot}4MeCN$ containing well-separated anions. The conversion of $[VO(edt)_2]^{2-}$ to $[V_2(edt)_4]^{2-}$ is thus established, but the reason for the incomplete conversion is unclear; the EtOH molecules may be interfering by mopping up reducing equivalents. Addition of excess NaACN leads to a messier reaction and a mixture of products. Further investigation of this reaction must await a nonsolvated form of a $[VO(edt)_2]^{2-}$ salt, but none is currently available. Nevertheless, available results are encouraging and the generality of the NaACN/H^+ reduction procedure for converting VO^{2+} to $[V-O-V]^{4+}$ or non-oxo V(III) species warrants further investigation with other VO^{2+} starting materials, of which there is truly no shortage in the established chemistry of this oxidation level.

Acknowledgment. This research was supported by the donors of the Petroleum Research Fund, administered by the American Chemical Society, and by NSF Grant CHE 8507748. We thank the Bloomington Academic Computing Service for a gift of computing time. We also thank Brian K. Conroy for his assistance in the molecular orbital calculations.

Supplementary Material Available: Tables S1–S4, listing fractional coordinates, isotropic and anisotropic thermal parameters, and bond distances and angles (8 pages); a table of calculated and observed structure factors (10 pages). Ordering information is given on any current masthead page. A complete MSC structure report (No. 86016) is available on request from the Indiana University Chemistry Library.

Notes

Contribution from the Twin Cities Research Center,
Bureau of Mines, U.S. Department of the Interior,
Minneapolis, Minnesota 55417

A New Reaction of Cyanide with Peroxide and Thiosulfate at pH 7–9

Joseph E. Schiller*

Received April 27, 1983

During research on a method to treat cyanide-containing waste waters, we investigated the reaction of H_2O_2, $S_2O_3^{2-}$, and cyanide[1] at pH 7–9 that produces thiocyanate and sulfate. To our knowledge, this reaction has not been reported previously. When only H_2O_2 and $S_2O_3^{2-}$ were reacted together (each at $(2.5-10) \times 10^{-3}$ M), a mixture of SO_4^{2-} and $S_4O_6^{2-}$ was produced; low pH and excess $S_2O_3^{2-}$ favored $S_4O_6^{2-}$ formation. The literature erroneously reports $S_3O_6^{2-}$ as the product in neutral solution,[2] while acidic and basic conditions lead to $S_4O_6^{2-}$ and SO_4^{2-}, respectively. Stoichiometric data in this work as well as TLC[3] confirmed that a mixture of SO_4^{2-} and $S_4O_6^{2-}$, not $S_3O_6^{2-}$, was formed. Either H_2O_2 or $S_2O_3^{2-}$ alone reacts with cyanide at an insignificant rate under the conditions used in this work.[4,5] When cyanide was present (8×10^{-4} M or less), H_2O_2 and $S_2O_3^{2-}$ reacted at about the same rate as when cyanide was absent. However, each mole of $S_2O_3^{2-}$ that reacted converted 1 mol of cyanide to SCN^- and yielded 1 mol of SO_4^{2-}. As the cyanide content decreased below about 5×10^{-4} M, parallel reactions to give SCN^-, SO_4^{2-}, and $S_4O_6^{2-}$ were observed until the cyanide was completely gone.

To define the mechanism, H_2O_2 and $S_2O_3^{2-}$ were first studied without cyanide present. Solutions of H_2O_2 and $S_2O_3^{2-}$ (1 L each) were prepared, thermostated at 25 °C, and separately adjusted to the desired pH value. After they were mixed to initiate the reaction, the pH was maintained with standard acid or base. Every 5–10 min, 50-mL aliquots were withdrawn for determination of $S_2O_3^{2-}$ and H_2O_2 by classical iodimetric titration.[6] If the titrations were done rapidly, mutual interference was less than 1%. Experimental data points for concentration and time were computer fitted to a third-order polynomial that calculated instantaneous concentrations and reaction rates for $S_2O_3^{2-}$, H_2O_2, and H^+ throughout the reaction. Table I gives the initial concentrations and rates that were calculated by using the polynomial. Reactions 1 and 2 proceeded in parallel according to the results shown in

$$S_2O_3^{2-} + 4H_2O_2 \rightarrow 2SO_4^{2-} + 3H_2O + 2H^+ \qquad (1)$$

$$2S_2O_3^{2-} + H_2O_2 + 2H^+ \rightarrow S_4O_6^{2-} + 2H_2O \qquad (2)$$

the right-hand column of Table I. Simultaneous equations using the stoichiometry[7] in reactions 1 and 2 and the calculated rate

---

* Address correspondence to Materials Processing Corp., 185 LaFond Ave., St. Paul, MN 55103.

(1) At pH 7–9, cyanide exists primarily as HCN with some free CN^- in equilibrium. The term "cyanide" means total cyanide rather than only free CN^- ion.

(2) (a) Tarugi, N.; Vitali, G. *Chim. Ital.* **1909**, *63*, 2929. (b) Lunenak-Burmakia, V. A.; Gerasenkova, A. N. *Zh. Neorg. Khim.* **1964**, *9*, 270; *Chem. Abstr.* **1964**, *60*, 9965*e*.

(3) Marchant, W. N.; May, S. L.; Simpson, W. W.; Winter, J. K.; Beard, H. R. *BuMines IC 8819*, **1980**, 20 pp. *Inf. Circ. U.S. Bur. Mines* **1980**, *IC 8819*, 1–20.

(4) Davis, R. E. *J. Am. Chem. Soc.* **1962**, *66*, 956.

(5) In control experiments, reactions of 1×10^{-2} M H_2O_2 with 8×10^{-4} M cyanide at pH 7, 8, and 9 had half-lives for cyanide disappearance of about 1000, 500, and 100 h, respectively. Masson, O. *J. Chem. Soc.* **1907**, *91*, 1449.

(6) Each 50-mL aliquot was analyzed for both $S_2O_3^{2-}$ and H_2O_2 by titrating first with standard I_3^- at pH 4 using starch indicator. Then H_2SO_4, KI, $(NH_4)_2MoO_4$ were added so that H_2O_2 would liberate 1 equiv of I_2 that was titrated with standard $S_2O_3^{2-}$ solution.